FMCW Radar With Enhanced Resolution and Processing Time by Beam Switching

PASCUAL D. HILARIO RE [1], **DAVIDE COMITE** [2] **(Senior Member, IEEE),**
SYMON K. PODILCHAK [3] **(Member, IEEE), CRISTIAN A. ALISTARH** [1] **(Student Member, IEEE),**
GEORGE GOUSSETIS [1] **(Senior Member, IEEE), MATHINI SELLATHURAI** [1] **(Senior Member, IEEE),**
JOHN THOMPSON [3] **(Fellow, IEEE), AND JAESUP LEE** [4]

[1]Institute of Sensors, Signals, and Systems, School of Engineering and Physical Sciences, Heriot-Watt University, Edinburgh EH14 4AS, U.K.
[2]Department of Information Engineering, Electronics and Telecommunications, Sapienza University of Rome, 00181 Rome, Italy
[3]The Institute for Digital Communications, School of Engineering, University of Edinburgh, Edinburgh EH8 9YL, U.K.
[4]Samsung Advanced Institute of Technology, Samsung Electronics Company Ltd., Seoul 2620, South Korea

CORRESPONDING AUTHOR: S. K. PODILCHAK (e-mail: s.podilchak@ed.ac.uk)

ABSTRACT We present the design of a novel K-band radar architecture for short-range target detection. Applications include direction finding systems and automotive radar. The developed system is compact and low cost and employs substrate-integrated-waveguide (SIW) antenna arrays and a 4×4 Butler matrix (BM) beamformer. In particular, the proposed radar transmits a frequency modulated continuous-wave (FMCW) signal at 24 GHz, scanning the horizontal plane by switching the four input ports of the BM in time. Also, in conjunction with a new processing method for the received radar signals, the architecture is able to provide enhanced resolution at reduced computational burden and when compared to more standard single-input multiple-output (SIMO) and multiple-input multiple-output (MIMO) systems. The radar performance has also been measured in an anechoic chamber and results have been analyzed by illuminating and identifying test targets which are 2° apart, while also making comparisons to SIMO and MIMO FMCW radars. Moreover, the proposed radar architecture, by appropriate design, can also be scaled to operate at other microwave and millimeter-wave frequencies, while also providing a computationally efficient multi-channel radar signal processing platform.

INDEX TERMS Automotive radar, multiple-input multiple-output (MIMO) radar, short-range radar (SRR), substrate-integrated waveguide (SIW), Butler matrix.

I. INTRODUCTION AND MOTIVATION

IN THE last decade, there has been an increasing demand for low-cost and low-profile radar solutions for short-range collision avoidance systems. Radar technology is becoming a standard equipment for the current generation of city cars and a key element for the design of next-generation self-driving platforms. One major challenge in this field is the possibility of achieving high angular resolution while maintaining relatively small processing times and reduced system complexity.

The use of multiple-input multiple-output (MIMO) techniques to provide real-time collision-avoidance information by means of millimeter-wave radars has also been under discussion over many years (see, e.g., [1]–[8]) but, even if very high resolution can be achieved by implementing well-established signal processing techniques [9]–[13], the

processing time can become an important issue for automotive radar applications and new self-driving systems [6], [7], [14]–[16].

Other high-resolution algorithms have also been studied to complement these approaches. For example, in [17] a MIMO system in conjunction with a multiple signal classification (MUSIC) [18] approach was reported. Capon filtering [19] and the estimation of signal parameters via rotational invariance techniques (ESPRIT) [20], have also been used in MIMO systems (more information can be found in [6] and [21]). On the other hand, super-resolution algorithms [22]–[24] generally perform better in terms of angular resolution since they search sub-spaces for the strongest signal, however this requires extensive time to process in the presence of multiple sources. Hence, delay-and-sum beamforming is generally less complex and computationally demanding to obtain the angular target response, even if it provides reduced angular resolution [25].

This type of low-resolution algorithm can detect multiple targets with reduced accuracy within the radar field-of-view (FOV). This can be extremely dangerous in automotive systems and for moving vehicles. For example, when a pedestrian is walking on the sidewalk in a narrow street or even when the car is traveling within a tunnel, targets can be misidentified. Multipaths can also represent an issue as they could generate false targets; i.e., they should be removed from the target image by performing additional processing (see, e.g., [26], and refs. therein). Considering those advancements, it should be mentioned that multipath propagation effects are not considered further herein as false targets are typically generated by low-resolution systems and in the presence of reflections from very long surfaces (guardrails for example). This means that the position of the ghost targets are typically outside the trajectory of the vehicle where the radar is mounted.

When considering broad FOV requirements, radars can employ phased-array techniques, beam switching, or frequency scanning antennas. Even if phased arrays are suitable for real-time beam scanning they can also require high implementation costs as well as cumbersome feeding networks, and can suffer from high losses [27], [28]. Frequency scanning antennas, instead, are moderate in complexity and cost, and can be easily integrated with frequency-modulated continuous wave (FMCW) radar systems [29], [30]. Likewise, the beam pattern of phased-array antennas, as well as frequency scanning antennas, can also be non-uniform and dispersive. The gain can also be reduced at larger scan angles, affecting the FOV [31], [32]. In these cases, since the gain can be non-uniform, a dependency on the power transmitted can be observed, influencing the target detection as a function of both angle and range. To compensate for such a non-constant gain profile, more complex approaches can be adopted such that the gain versus angle is more stable. Alternatively, techniques based on switched beamforming networks can represent an attractive solution [33]. They can be considered a compromise
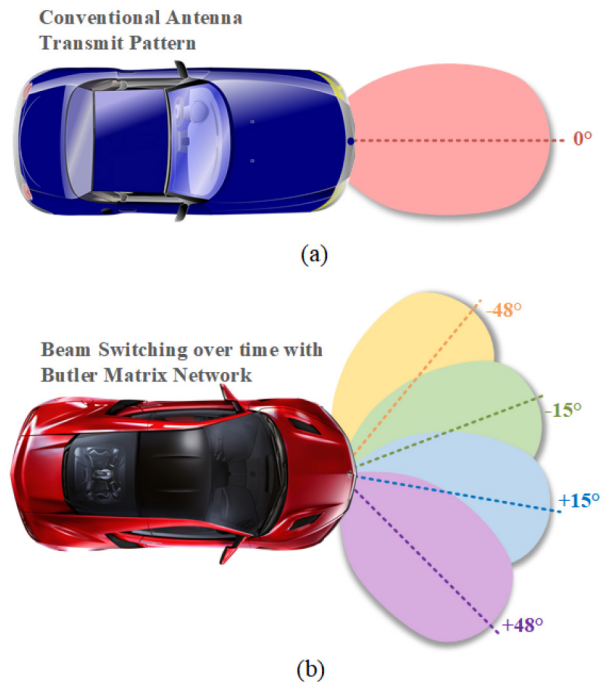

FIGURE 1. Possible radar configuration for automotive systems; comparison between a conventional radar front end (a) with the proposed RF beam steering approach based on a BM network (b) showing a wider illumination angle when considering all the transmitted beam patterns.

between cost and complexity, while maintaining close-to-ideal antenna beam patterns for the switching angles [33].

To provide short processing times at reduced cost and complexity, this paper presents the design and test of an FMCW radar for automotive applications, proposing beam switching at the transmitter (see Fig. 1) for enhanced FOV. A preliminary investigation of our proposed radar architecture has been reported in [34], [35], and [36]. The advanced system, now detailed in this paper herein, provides faster processing and enhanced resolution as well as higher antenna gains, improving the possible radar range and detection capabilities at the extremities of the FOV. Basically switched time-domain beamforming at the transmitter is implemented, in conjunction with pattern-multiplication and multi-channel processing at the receiver, to achieve high resolution angular target detection.

The newly developed radar system also employs a Butler matrix [37], i.e., a passive radio-frequency beamforming network in transmission, as in [38], but now with sum-and-delay processing at the receiver whilst being demonstrated with said transmitter and radar electronics for a low-profile implementation. High angular resolution and broad FOV are achieved with reduced processing time ($< 40\,\mathrm{ms}$), providing therefore, and as will be shown in the paper, advanced performance with respect to comparable SIMO and MIMO radar systems. These features, in conjunction with the newly reported signal processing methodology described in the following, makes the proposed radar architecture particularly suitable for collision-avoidance automotive systems as well
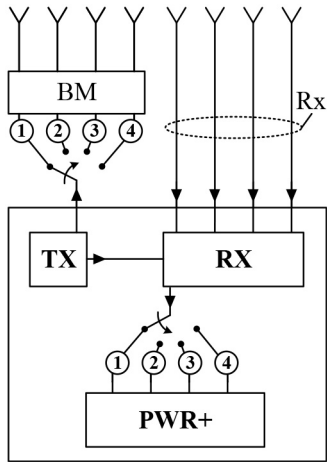
FIGURE 2. Schematic representation of the proposed BM radar system. Each of the 4 states of the switch are individually processed (see the *Power Plus*, *Pwr+*, module), providing parallel computation as shown in Figs. 3 and 5(c).

as other real-time tracking scenarios which require enhanced resolution.

II. STATE OF THE ART AND THEORETICAL BACKGROUND

In [34], a radar system comprised of conventional substrate-integrated-waveguide (SIW) transmit antennas based on a 2×4 MIMO system was proposed. That system suffered from gain degradation for angles off broadside. Moreover, the processing time required for MIMO operation was higher than our proposed system (i.e., the proposed radar system is outlined in Figs. 2 and 3). In [35] the same beamformer as the one presented here, i.e., in Fig. 2, was briefly examined, but that work only reported comparative studies of the transmit gain with respect to other MIMO and SIMO radar arrangements. In [36], also, four independent 2×4 MIMO sub-modules were used and combined together with a multiplication technique which was shown to improve the radar accuracy by reducing the side-lobe level (SLL). However, the system required a complicated hardware setup and involved signal processing. This is because each of the four radar sub-modules needed to process a 2×4 MIMO acquisition individually, which is not needed in this paper, due to the developed radar signal processing approach, defined as *Power Plus* (*Pwr+*). This technique, *Pwr+*, will be further described shortly.

The use of lens antennas, on the other hand, can improve the gain, FOV, and the angular resolution but at the cost of increased size [39]–[42], making those solutions less practical to be fitted onto a vehicle. This problem was partially mitigated in [43] introducing a metasurface, whose thickness and weight of the lens were significantly reduced compared with a more conventional planoconvex dielectric lens antenna. However, the total size of the lens antenna is still bigger with respect to the system proposed in this work.

A. FMCW RADARS, PATTERN MULTIPLICATION & ANGLE ESTIMATION

FMCW radars are based on the transmission of a CW signal over a fixed period of time, introducing a frequency modulation on the signal, which can periodically increase or decrease over time [29], [44]. These radar systems can calculate the range position of the illuminated target, with an accuracy that is comparable with the wavelength of the probing signal. In contrast with a conventional pulsed radar system, FMCW radars do not require the use of high peak power and can simplify the realization of the required processing circuits [29], [44].

In order to retrieve the angular position of the scattering objects with respect to the radar location, at least two receiving antennas are needed. A system not in mechanical rotation, formed by 1 transmitter and 2 receivers (placed at a distance d), constitutes a basic single-input multi-output (SIMO) radar. By assuming that one of the two antennas collects a signal from a direction over the horizontal plane given by θ, an additional distance equal to $d \sin \theta$ should be considered to reach the second antenna. This corresponds to a phase difference of $\beta = (2\pi/\lambda)d \sin \theta$ between the received signals. On this basis, it is possible to determine the angular position of the target through the following simple expression:

$$\theta = \arcsin\left(\frac{\beta\lambda}{2\pi d}\right) \quad (1)$$

For classic beamforming algorithms, such as the Barlett beamformer, the raw data at the sensor nodes are adjusted in order to account for the delay caused by the travelling wavefront [18]. Some of the outputs are weighted to account for the antenna configuration. This means that the signals are constructively interfering in order to detect the direction of maximum energy. The resulting pattern can be perhaps associated with the shape of a *sinc* function, or in other words, to a function that has a Gaussian pattern with the point of maximum return occurring at the peak of the target. This approach can also be used as a basis for a more refined signal processing method to combine the RF channels or views (see Figs. 2 and 3) as employed in this work. Also, as investigated in [36], a more accurate radar response of the targets occurs when multiple images of the same target are convolved in the time domain. Basically, this operation has a smoothing effect which better identifies target peaks in the angular spectrum estimate.

This underlying principle can be applied also for the proposed BM radar system and its *Pwr+* signal processing of the multiple RF channels (as illustrated in Figs. 2 and 3). Let us define $E(f)$ as a sinc-shaped function in the frequency domain:

$$E(f) = sinc(2\pi f\ T) \quad (2)$$

where T is the period of the function, f is the frequency of the signal. And a smoothing function with the same shape:
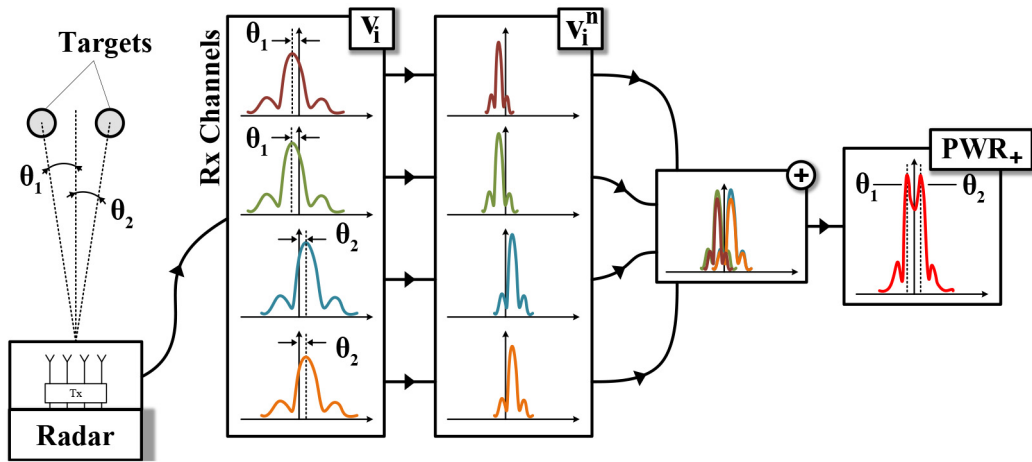
$$W(f) = sinc(2\pi f\ T) \quad (3)$$

FIGURE 3. General operation of the proposed *Pwr₊* radar signal processing algorithm for the four channels. Two targets located at θ_1 and θ_2 are considered. Each channel for the different angular views is multiplied *n* times and then combined. The resulting angle target estimate plot is shown in red for the four combined channels.
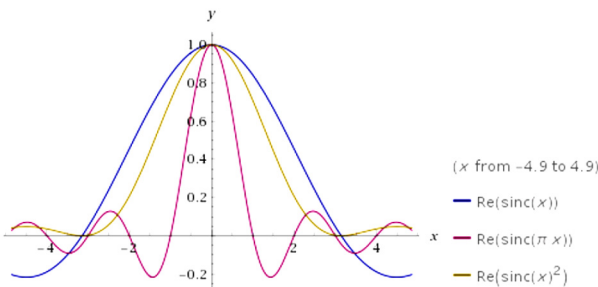

FIGURE 4. Results of spectral multiplication for Gaussian functions in the frequency domain as a pre-requisite for the adopted *Pwr₊* radar signal processing approach for the combination of multiple channels (see Fig. 3).

Their convolution in the time domain will result in a multiplication in the frequency domain. This will be defined as:

$$E'(f) = E(f) \cdot W(f) = sinc^2(2\pi f\ T) \qquad (4)$$

So if the processing of the four states of the BM radar system can be used in conjunction with multiplication of the angular spatial spectrum (see Fig. 3), this will result in a smoothing process as illustrated in Fig. 4. Basically this defines a sharper peak for the target estimate. More information about this smoothing process, pattern sharpness, and the supporting mathematics can be found in [45]. As will be further examined in the paper, this technique which employs these mathematical concepts (defined as the *Pwr₊* radar signal processing approach) can improve radar accuracy and image sharpness, due to the noted pattern multiplication operation.

A SIMO system can only provide a coarse angular resolution, defined by the half-power beamwidth, Θ_{3dB}, of the receiving array. A way to increase the angular resolution consists in increasing the number of receivers and/or the distance between them. The latter strategy, however, introduces grating lobes, thus limiting the angular range (i.e., the FOV) of the radar, derived from (1) considering the maximum phase difference (i..e, π and $-\pi$), as $\theta_{FOV} = \pm \arcsin(\frac{\lambda}{2d})$.

The angular resolution is set by the IEEE Standard for Radar Definitions [46]: "The ability to distinguish between two targets solely by the observation of their angle, usually expressed in terms of the minimum angle separation by which two targets at a given range can be distinguished." It is often assumed that the two targets to be identified have the same received power level (usually the half-power point), and minimum angular separation, which thus constitutes the angular resolution. An estimation of this parameter is dependent on the size of the antenna aperture [47]: $\sin(\theta_{RES}) \approx \lambda/D$, D being the size of the receiver. This approach, unfortunately, unavoidably increases the number of RF chains based on the number of receiver elements.

B. MIMO RADAR

To reduce the number of receiving chains needed to support the use of more antennas, MIMO systems have been proposed (see, e.g., [1], [48]). They require the use of more transmitters to provide higher resolution at reduced costs with respect to a SIMO system. By increasing the number of transmitters, indeed, the number of virtual receivers is given by $N_{Tx} \times N_{Rx}$. Therefore, when element spacing is appropriate, a 2×4 MIMO radar would provide the same angular resolution as a 1×8 SIMO radar.

Typically the transmitters are activated sequentially in time, so that, when the first radiates, the target reflects back a signal with a phase distribution at each receiver element given by 0, β, 2β, and 3β. Once the received signal has been stored, the second transmitter is activated and a phase offset of 4β is observed with respect to the first transmitted signal. This offset will contribute to the second half of the virtual receiving array (with phases 4β, 5β, 6β, and 7β, respectively). Once the returned signals for both halves of the array have been collected, considering $\lambda/2$ spacing for the effective virtual array, the returned signal is processed as a single eight-element receiver array. It should be mentioned that having transmitters and receivers co-located in space can make the physical dimensions of the MIMO radar significantly smaller. This would reduce the hardware costs
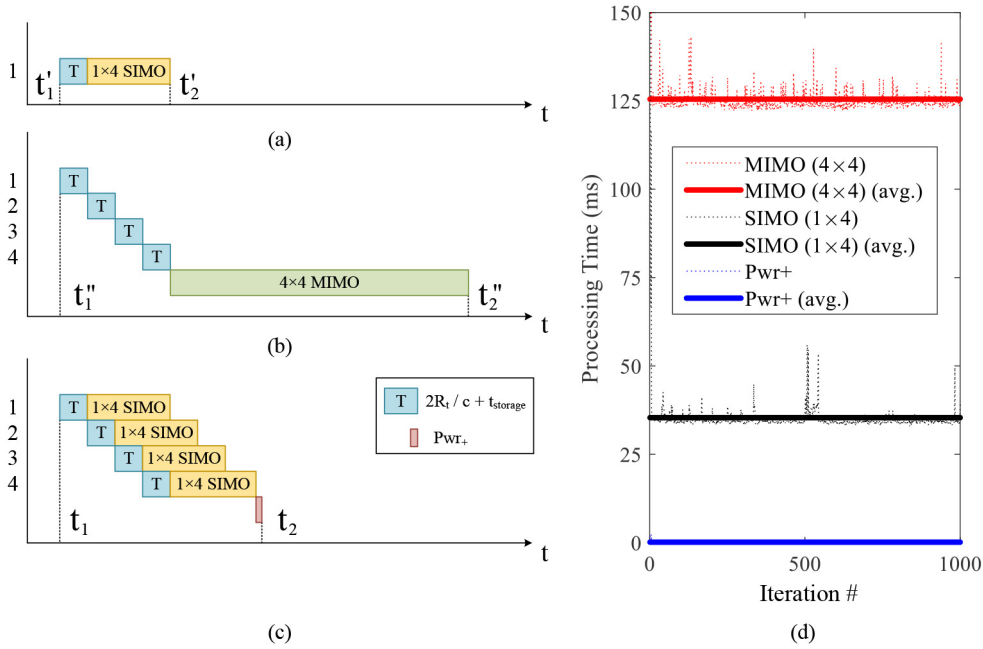
FIGURE 5. Timing sequence diagram for the proposed radar when compared to more conventional approaches: (a) 1 × 4 SIMO, (b) 4 × 4 MIMO, and (c) the proposed *Pwr*+ approach. (d) Processing time estimation for each of the three cases based on MATLAB calculations. In particular, the horizontal axis is the iteration number defining the number of times the radar measurements were completed automatically and then individually processed in MATLAB. This was required in order to estimate the mean processing time for each individual radar setup providing a comparison for the different radar systems.

while maintaining high resolution, at the expense however of the processing time.

III. BUTLER MATRIX FMCW RADAR

To achieve the same performance of a MIMO system or better, but with reduced computational complexity, we propose here a radar system connected to a 4×4 BM, providing four possible phasing configurations at the transmitting point. The system architecture is shown in Fig. 2. The BM is connected to a single transmitter array, which is associated with one transmission channel and four receiving channels. This transmitter generates four different beams in time (see Fig. 3) depending on the port excited. The complete transmitter antenna system, therefore, is constituted by a single-element antenna array, time-domain switch, and BM beamformer.

The four different angular views (i.e., the beams) divide the observed space in four sections, which are combined in post-processing through a technique further defined here as *Pwr*+ (i.e., *Power Plus*, which refers to the power and addition operations made in the processing as further described in the next sub-section). After, the delay-and-sum beamforming is applied for each of the BM switching angles, the data is taken and a multiplication technique is applied to combine the individual angular target responses similar to [36]. As discussed in the following, this provides improved angular resolution along with competitive processing time.

A. SIGNAL PROCESSING USING PWR+ AND BUTLER MATRICES

The *Pwr*+ procedure is illustrated in Fig. 3, and it can be summarized as follows when considering the BM transmitter.

1) Both switches in Fig. 2 are synchronized to be at the same position (i.e., from 1 to 4). Then, the BM is excited through the first port, the scattered signals are collected by the 4 receivers and stored. Therefore, both switches are set on the subsequent position, and the signal is processed as a conventional 1×4 SIMO radar. It is noted that the *Pwr*+ block includes four independent processors, thus defining a parallel processing algorithm to avoid inefficient queues that would increase the total delay (see Fig. 5(c)). The process is repeated four times in sequence to collect the signal through all beams.

2) When the four datasets have been processed, the following combination algorithm is implemented (see Fig. 3):

$$v_{\mathrm{Pwr}_+} = v_1^n(\theta) + v_2^n(\theta) + v_3^n(\theta) + v_4^n(\theta) \qquad (5)$$

where v_i represents one of the four views, and n corresponds to a positive integer greater than 1, introduced to provide a sharper pattern for the single beam (see Fig. 4). This approach can obviously increase when more voltage channels are considered (set equal to four here for proof of concept).

The proposed processing makes the compound signal (i.e., v_{Pwr_+}) sharper and more defined, improving the accuracy over more conventional radars. This *Pwr*+ approach is original and has not been applied before in other works, to the best knowledge of the authors. We should make it clear that improved resolution is not achieved by the n multiplication

of the individual radar signals alone, v_i^n, but it is the combination (v_{Pwr_+}) of these four voltage channels which can offer improved resolution. This is because the individual returned signals offer different views or perspectives of the targets, similar to [4], within the FOV of the radar. As discussed next, shorter processing-time performances with respect to a comparable MIMO system can also be achieved.

B. PERFORMANCE ANALYSIS

To understand the temporal performance of the BM radar with respect to a conventional 4×4 MIMO system, we developed a numerical study to analyze the time delay of the processing. Three different configurations have been considered: a 1×4 SIMO radar, a 4×4 MIMO system, and the proposed BM radar. As mentioned, the latter could be considered as a 1×4 SIMO enhanced by the presence of four different beams, but without introducing additional RF chains. To operate the four channels, as shown in Fig. 2, every time a signal is detected, the transmitter is switched to the subsequent port of the BM.

Timing diagrams for the signal processing shown in Fig. 5(a, b and c) gives an estimation of the total delay. It starts accumulating when the transmitter sends the signal and it finishes when the information of the target position is acquired. In such diagrams, there are 4 different timing blocks.

1) T: time that starts when the transmitter begins sending the pilot signal in air. The signal hits the target and the time stops with the reception of the raw data at the receivers. It depends on the target distance (i.e., R_{t}) and on the time the receiver block takes to record and store the collected raw data (i.e., t_{storage}). Therefore, we consider

$$T = \frac{2R_{\text{t}}}{c} + t_{\text{storage}} \qquad (6)$$

Note that, since $t_{\text{storage}} \gg \frac{2R_{\text{t}}}{c}$, the term related to the target can be neglected.

2) 1×4 SIMO: time needed by the system to process the raw data and to obtain the information of the target position. The average value is equal to about 36 ms when developing the processing in MATLAB (version R2017b), as shown in Fig. 5(d) (black curve).

3) 4×4 MIMO: time needed by the system to process the raw data by following [6], [49]; once the four different signals have been collected by the four beams the average processing time was about 125 ms (see Fig. 5(d), red curve).

4) Pwr_+: time needed to apply the Pwr_+ algorithm right after the four views have been acquired by the system based on the BM, which perform four SIMO iterations. Basically, the average value of about 0.3 ms in Fig. 5(d) (blue curve) is needed for the multiplication.

The time estimations for each case were obtained running 1000 iterations on a code that performs the relevant radar

processing. The machine is equipped with an Intel Core i7-4790 CPU (3.60 GHz, 4 cores, and 8 logical processors), and 16 GB of RAM.

The total time required for each case is given in the following:

$$\Delta t_{\text{SIMO}} = t_2' - t_1' = T + t_{1\times 4} \approx T + 36 \text{ ms} \qquad (7)$$

$$\Delta t_{\text{MIMO}} = t_2'' - t_1'' = 4T + t_{4\times 4} \approx 4T + 125 \text{ ms} \qquad (8)$$

$$\Delta t_{\text{BMPwr}_+} = t_2 - t_1 = 4T + t_{1\times 4} + t_{\text{Pwr}_+} \approx 4T + 36 \text{ ms} \qquad (9)$$

Taking only into account the processing time term, computation times and angular resolutions are also compared in Table 1. As it can be observed in Fig. 2, the proposed BM radar is composed of 4 receiver elements, which therefore, will define an angular resolution of 30 degrees on their own. However, this resolution is based on a single view (1 out of 4), and when all the 4 views are processed using the Pwr+ algorithm (by Eq. (5)), a more refined angular resolution is made possible by the proper selection of n and the combination of the multiple channels by pattern multiplication.

Taking into account the three different scenarios under comparison (classic 1×4 SIMO, classic 4×4 MIMO and the proposed BM architecture), it can be observed that the BM system (i.e., $\Delta t_{\text{BMPwr}_+}$) is significantly faster than classic 4×4 MIMO (i.e., Δt_{MIMO}) whilst offering enhanced angular resolution and with simpler radar hardware implementation.

IV. BUTLER MATRIX AND ARRAY DESIGN

Both high angular resolution and broad FOV are important requirements for automotive applications. To scan the space in front of the radar a beamforming technique should be included. Typically, antenna arrays work on a finite number of discrete states, which are determined by the phase distribution applied to each element. We propose here the design of an SIW antenna array and feeding network based on the BM concept. Alternative approaches for the beamformer, such as the *Blass matrix* [50], the *Wullenweber array* [51], and lens antennas could also be adapted to this system.

A. BUTLER MATRIX

The BM provides uniform amplitude distribution and constant phase difference at its output ports [37]. It consists of N input and N output ports, with $N = 2^m$ and $m = 2, 3, \ldots$. A 4×4 BM is depicted in Fig. 6, which shows the three basic components: delay lines, crossovers, and 90° hybrid couplers. Typically, it is also possible to use 180° hybrids couplers, which would involve fewer delay lines, even if its positions and magnitudes would follow a more complicated
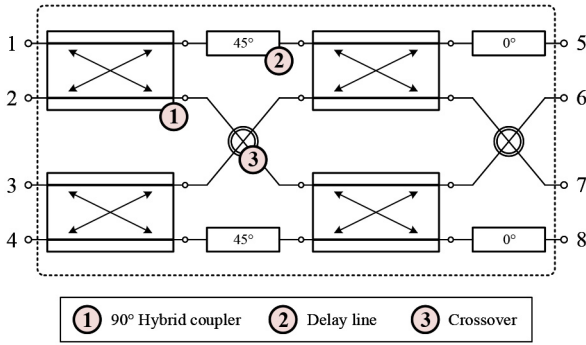
FIGURE 6. Schematic circuit representation of the proposed 4 × 4 BM, representing the radar antenna beamformer for the transmitter.

TABLE 2. Number of hybrids and delay lines required for an $N \times N$ BM.

Component	Rows	Columns	Total
Hybrid coupler	$N/2$	n	$n \cdot N/2$
Delay line	$N/2$	$n-1$	$(n-1) \cdot N/2$

TABLE 3. Phase outputs on a butler matrix.

Excited Port	[1]Output Phase (β)	[2]Beam Direction (θ_0)
1	+45	14.5°
2	-135	−48.6°
3	+135	48.6°
4	-45	−14.5°

[1] Phase difference between consecutive output ports (i.e. 5-6, 6-7 and 7-8).
[2] Beam direction in the far-field; the relation between β and θ_0 is given by Eq. 1 with array spacing $d = 0.5\lambda$, with $f = 24$ GHz.

pattern [52]. Once the network is sized, the number of delay lines and couplers can be easily obtained as outlined in Table 2.

Depending on the excited port, the resulting weights applied to the array controls the pointing direction for the transmitted signal. The output phase differences between consecutive ports and the corresponding direction of the induced main beams for a 4 × 4 BM are shown in Table 3. The delay lines connected on top and bottom and between the hybrids require a specific phase delay, which is related to N as follows [53]:

$$\phi_{dl} = 90° - \frac{1}{N}180° = 45°. \tag{10}$$

More details on advanced BM designs can be found in [53].

B. ANTENNA DESIGN IN SIW TECHNOLOGY

We describe here the design procedure of a planar waveguide slot array antennas [54], [55] to be connected with the four outputs of the BM. A standing-wave design [38], depicted in Fig. 7, has been selected and optimized by means of CST Microwave Studio. To achieve a broadside and symmetric beams the spacing between slots is set to $\lambda_g/2$ [56], whereas the distance between the last slot and the traversal vias is
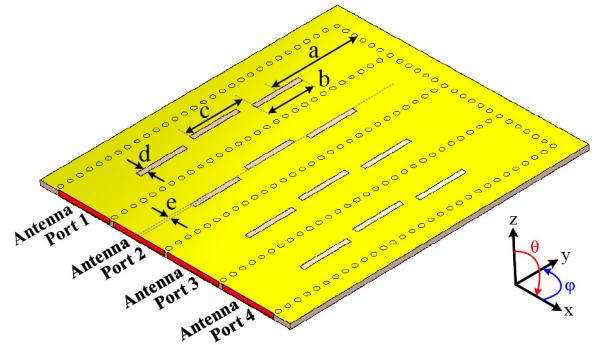

FIGURE 7. Simulation model of the SIW slot antenna array, defined by four 3 × 1 sub-arrays ($a = 9.28$; $b = 4.89$; $c = 6.10$; $d = 0.54$; $e = 0.28$ [mm]) for operation at 24 GHz. This SIW structure is representative of the radar antenna transmitter and receiver (albeit no beamforming network).

approximately $3\lambda_g/4$. A 3 × 1 four-element series-fed sub-array is considered as trade-off between the needed antenna gain over the plane parallel to the SIW structure (i.e., normal to the z axis in Fig. 7) and the encumbrance of the system.

The displacement for each slot from the axial center of the SIW along the x axis, the slot widths and the lengths (l_{slot}), have been finely tuned to cancel higher-order mode coupling, starting from an initial value given by $l_{slot} = \lambda_0/\sqrt{2(\varepsilon_r + 1)}$ [57]. Four sub-arrays are needed for the final design, leading to a 4 × 3 array, as shown in Fig. 7. The antenna dimensions determined by the optimization process are reported in the caption.

The simulated reflection coefficients at each port of the proposed SIW array, reported in Fig. 8(a), exhibit a −10 dB operational bandwidth of 7.3% (1.75 GHz). The simulated radiation and total efficiencies are also reported in Fig. 8(b), showing 85% over the operating band, reaching values over 90% around 24.75 GHz. A realized gain versus the frequency (not reported here) above 15 dB$_i$ has been achieved over the entire 1.75 GHz operating band.

The main lobe direction of the SIW series-fed slot array is a critical aspect for the considered radar application, since the phasing at each slot presents different values versus the frequency. The simulated main lobe direction (not reported here for brevity) over the frequency, in both the principal planes, showed very minor deviation with respect to broad-side (about 0.7° in the YZ plane; i.e.,$\phi = 90°$). The level of the first sidelobe was found to be around −13 dB within the XZ plane, and −23 dB for the YZ plane. The simulated radiation patterns over the E and H planes (not reported here for brevity), at three different frequencies (the two extremes of the frequency of operation and the center), show consistent results, which is a key aspect for a proper operation of the FMCW radar. Cross-polarization levels in excess of −25 dB are also achieved when compared to the main beam maximum. This confirms the suitability of the array performance for the proposed radar system.

C. BEAMFORMER DESIGN IN SIW TECHNOLOGY

We consider here a hybrid coupler based on the waveguide design proposed in [58]. Properly selecting the length L
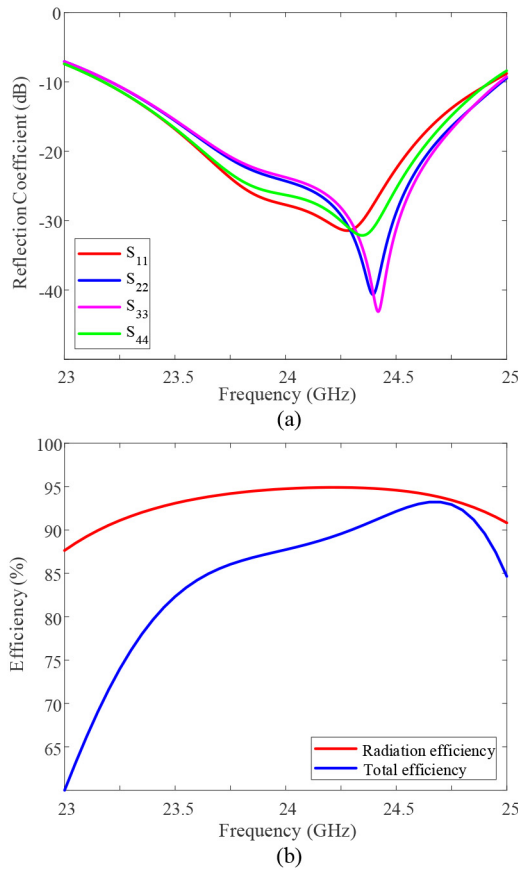
FIGURE 8. (a) Simulated reflection coefficient for the 4 antenna ports of the SIW 4 × 3 antenna array; (b) simulated radiation and total efficiencies considering uniform excitation of all the ports (see Fig. 7) for broadside radiation.
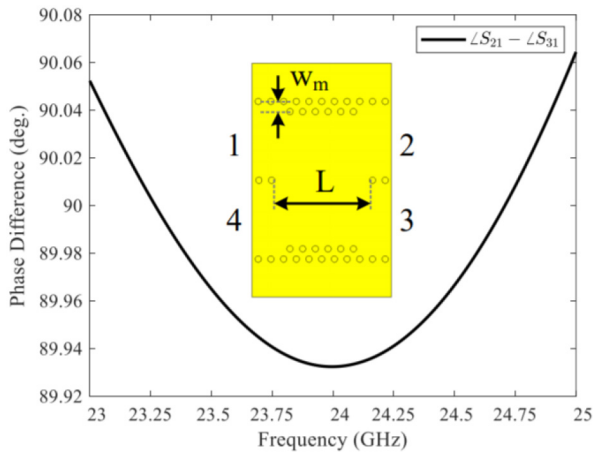

FIGURE 10. Additional passive circuit components for the SIW BM: (a) top view of the crossover conformed by 2 riblet short 90° hybrids (one highlighted by a red dashed line), (b) top view of the required SIW delay line, (c) SIW transmission line bends for improved connector matching, (d) exponentially tapered microstrip-to-SIW transition.

A very good output phase difference within the simulated bandwidth has been achieved, with maximum deviation in the order of 0.1°, as reported in Fig. 9.

For the design of the crossover, two cascaded couplers are used as in Fig. 10(a). This is possible given the split and combining characteristics of the 90° hybrid coupler: when port 1 is excited, at the two outputs of the first hybrid (red dashed square) a 90° phase difference is obtained. Therefore, at the second hybrid two ports are excited simultaneously, performing as a combiner and outputting all the signal through port 3. In other words, in the second stage, the hybrid works in reverse with respect to the first. Simulated results (not reported here for brevity) testify an excellent matching, high isolation, and insertion losses of about 0.2 dB. With respect to the required delay lines, 90° bends have been used including vias on each of the corners for matching purposes [60]. Moreover, phase-delay adjustments for this component are made by tuning l_{delay}, which is depicted in Fig. 10(b).

Since the SIW width is narrower than the actual connector width, a transition was designed. Figure 10(c) shows the input SIW paths followed by each individual port. In this case, unlike the SIW delay lines, 90° curvatures [60] were chosen instead of 90° bends to optimize the matching performance. This is likely related to the proximity of the input ports of the BM, which makes this area more sensitive to the input impedance. It should be noted that these different paths had to be properly adjusted to avoid unwanted phase offsets at the sub-arrays. The transition from microstrip to SIW has been designed following an exponential tapering (see Fig. 10(d)), as proposed in [61].

A picture of the manufactured BM is shown in Fig. 11. Simulations and measurements of the amplitude balance for each of the four states are reported in Fig. 12. The output phase differences are shown in Fig. 13. A very good matching can be observed between simulations and measurements (below 5°), for each of the different beam switching states.

FIGURE 9. Simulated output phase difference for the 90° SIW hybrid coupler employed within the BM. A top view of the SIW coupler is shown in the inset where the ports are defined.

in Fig. 9, the power split through the output ports 2 and 3 experiences a phase difference of 90°. To provide good matching and to balance the power splitting [59], the value of w_m has been tuned. Simulation results (not reported here) exhibit low insertion losses within the operating bandwidth (around 0.2 dB) and a very high isolation (below 30 dB).
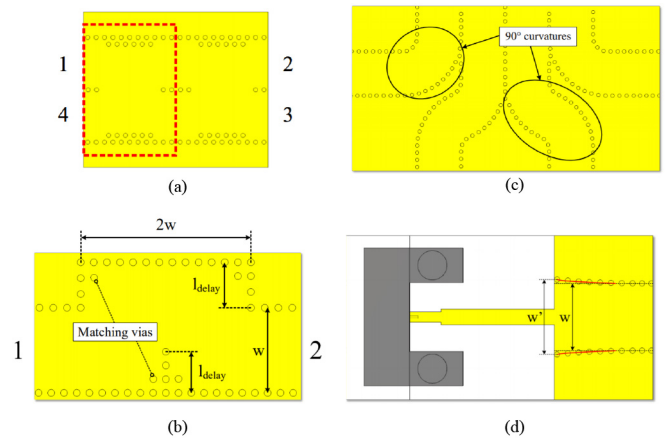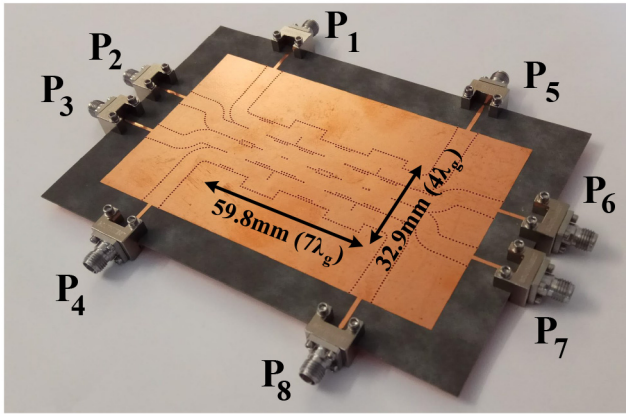
FIGURE 11. Photograph of the prototyped BM prior to integration with the antenna and radar. Ports from 1 to 4, i.e., P_{1-4}, corresponds to the input and 5 to 8, i.e., P_{5-8}, to the outputs.

D. BEAMFORMER AND ANTENNA ARRAY INTEGRATION

The manufactured beamforming system and the planar array have been integrated as reported in Fig. 14. Radiating slots were etched in the top ground plane to avoid unwanted coupling coming from the microstrip sections at each port. The simulated and measured reflection coefficients within the relevant bandwidth are reported in Fig. 15(a), showing values below −10 dB. The four normalized radiation patterns, achieved by switching the driven ports, are reported in Fig. 15(b). A very good agreement between the simulated and measured steered patterns is observed. Due to constraints enforced by the NSI near-field scanner used to collect antenna measurements, results only cover an angular range from −60° to 60° over the ZX plane in Fig. 15.

V. RADAR SYSTEM TESTING AND RANGE ESTIMATION

In order to test the capabilities of the proposed radar system, a set of measurements have been performed in a calibrated anechoic chamber at Heriot-Watt University. Fig. 16(a) shows the proposed butler matrix array (BMA), which acts as transmitting system for the radar. Results have been collected manually by switching the ports of the BMA and terminating the others with 50-Ω loads. Also, to ensure low-cost demonstration and implementation of the supporting radar materials (i.e., dielectric laminates, radio-frequency beamforming networks, and the supporting electronics), the FMCW system operated at 24 GHz with a 250 MHz bandwidth. The radar transmitter and receiver PCBs could also be scaled downwards in size to operate at 77 GHz (following the standard tolerancing available from PCB manufactures) while different radar electronics could be properly selected as well. This 77 GHz operational frequency range represents another standard carrier frequency for automotive applications.

The SIW 4×3 array shown at the bottom of Fig. 16(a) constitutes the receiving antenna. In this case, only the four central elements of the antenna array have been used, realizing the architecture described in Fig. 2. The
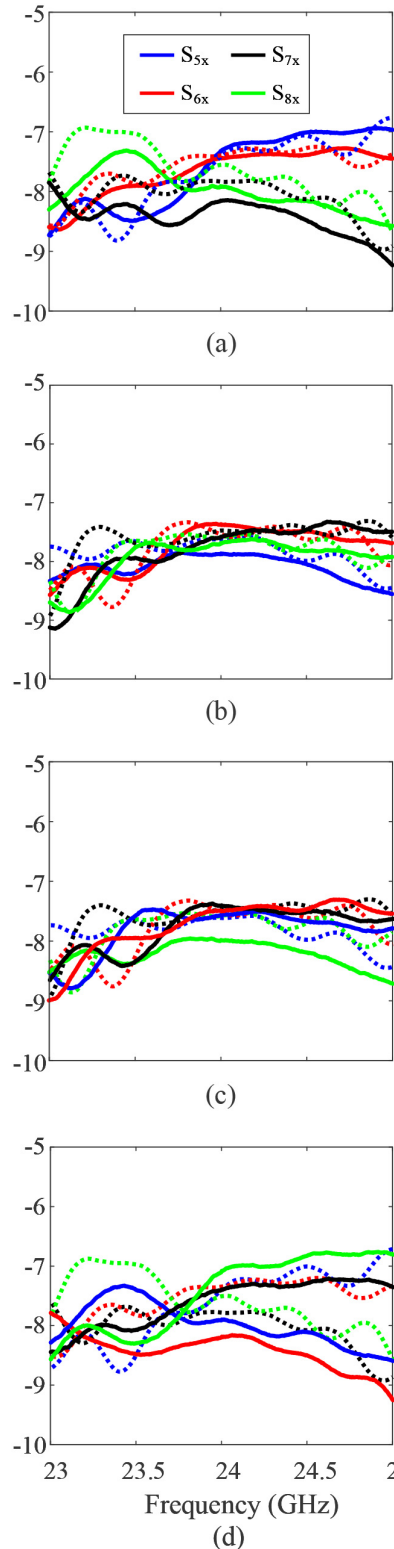

FIGURE 12. Simulated and measured S-parameters for the SIW BM as in Fig. 11. Results are shown when each individual input port (1-4) is excited: port 1 (a), port 2 (b), port 3 (c) and port 4 (d). Dashed lines correspond to simulations and solids lines to measurements.

employed radar system electronics used connectorized monolithic microwave integrated circuit (MMIC) components from Analog Devices containing the phase-lock loop and
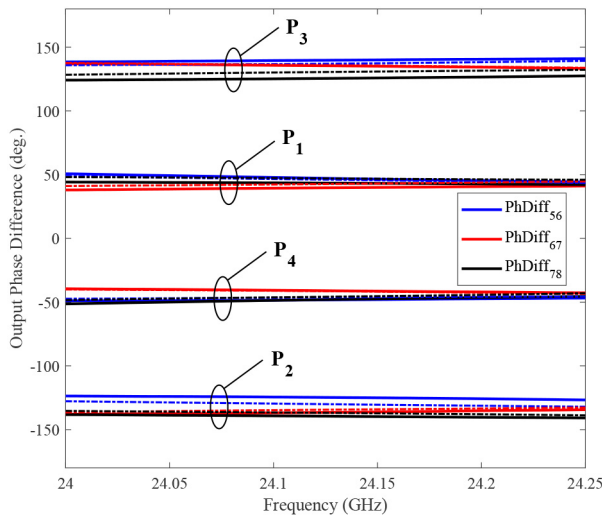
FIGURE 13. Simulated and measured phase difference for the SIW BM (see Fig. 11). Dashed lines correspond to simulations whereas solid lines relate to measurements. Phase differences are defined between consecutive output ports (5-8) when each individual input port (1-4) is excited. Each of the obtained output phase states match the expected values as they are shown in Table 3.
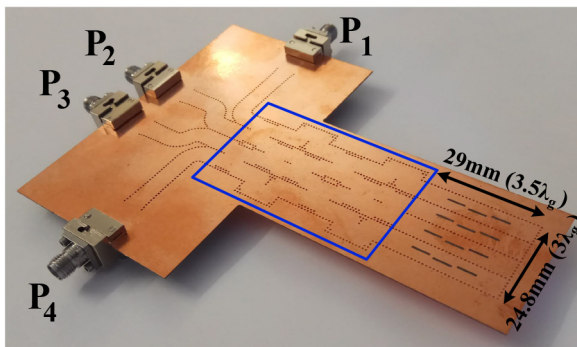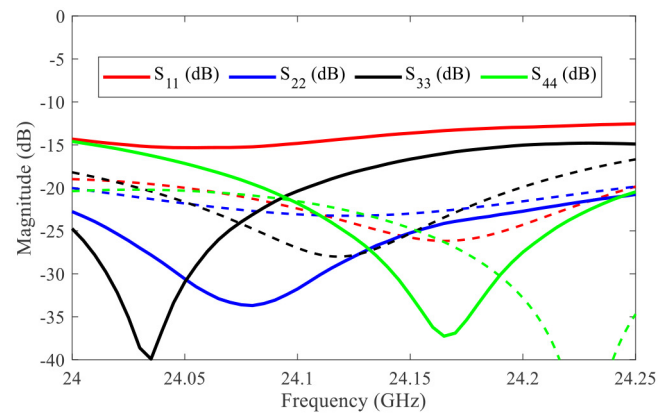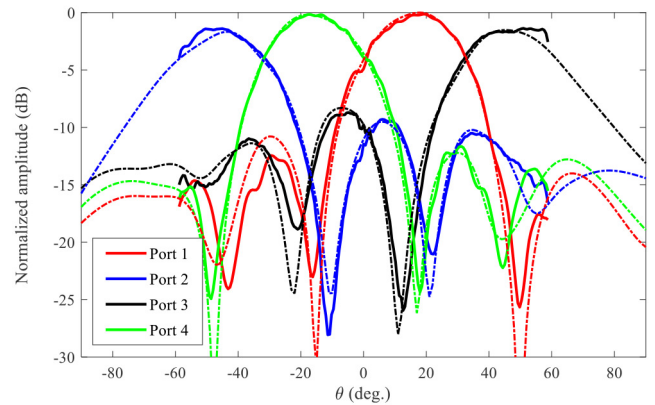

FIGURE 14. Picture of the manufactured SIW BM and antenna array defining the radar transmitter.

FIGURE 15. Simulated and measured reflection coefficients (a) and the steered beam patterns (b) for the radar antenna transmitter (see Fig. 14) normalized to the observed maximum. Dashed lines correspond to simulations while solid lines relate to measurements.

voltage-controlled oscillator (ADF4159), the transmitter chip (ADF5901), and a 4-port receiver chip (ADF5904). Data sampling was performed using the ADAR7251, a 4-channel continuous time analogue to digital converter (ADC) with 16-bit resolution. This enabled fast acquisition for the down-converter at receive. Also, each of the receiver antenna ports were connected to an HMC751LC4 low noise amplifier (LNA) also from Analog Devices to reduce system noise (see [35, Fig. 2] for a representative circuit schematic). Raw datasets collected at the receivers were then post-processed in MATLAB. The measurements were made at a range equal to about 2 meters using metallic targets; i.e., the two vertical metallic posts shown in Fig. 16(b) which could be made to have different angular separations.

The measurement procedure and results are described in the following. It should be highlighted that two targets were selected and appropriately spaced to ensure an angular resolution beyond the capability of the four-element SIW receiver. This θ_{RES} can be calculated to be 30° considering the employed $\lambda/2$-spaced receiver; i.e., four sub-arrays

defined by a four-element 3×1 series-fed array in SIW technology (see Fig. 7). As described previously, a similar radar system was reported in [35] where additional measurements were also compared to more conventional (and equivalent) SIMO and MIMO radar configurations [34]. It was shown in [35] that the proposed BM radar architecture can offer improvements in terms of higher returned signal powers, improved signal-to-noise ratios, and enhanced FOV (see [35, Figs. 6 and 7]).

During the measurements for this paper each port of the BMA was individually driven and returned signals were sampled at the radar module, as discussed in Section III-B. These results were then processed as an individual SIMO radar because the transmitted beam was steered to a particular direction as defined in Table 3. Once the four beams were transmitted and the four received signals obtained, the Pwr_+ algorithm described in Section III was applied to the four receiver channels. However, since each individual view shows an angular resolution above the angle between the two targets; i.e., $\theta_{\text{RES}} = 30°$, the resulting view will only show one peak (see gray lines in Fig. 17). More views can be anyway added considering space constraints, implementation costs, and a more advanced beamformer.

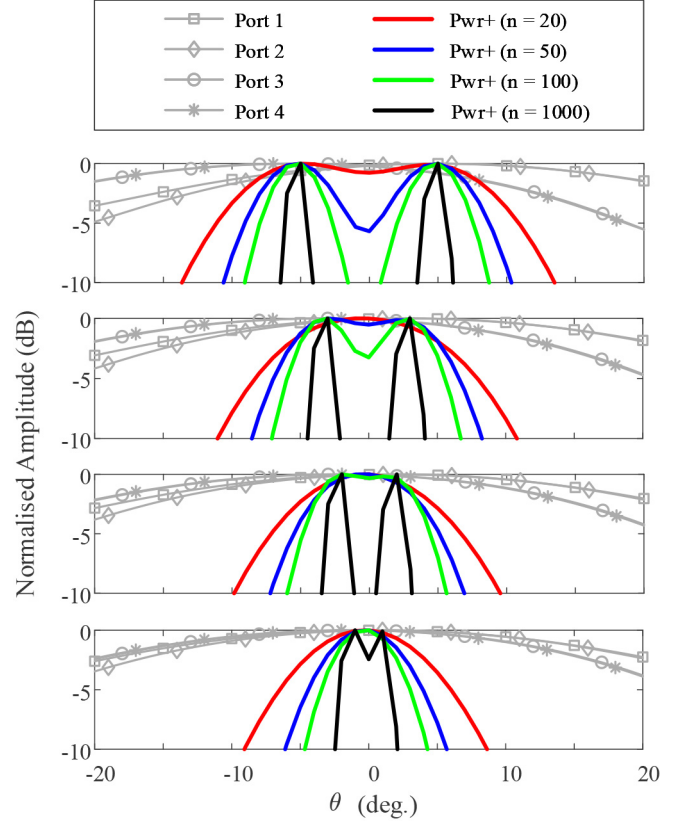**TABLE 4.** Comparison of a 4 × 4 MIMO radar with the proposed BM radar.

	4 × 4 MIMO	PWR+ (n = 20)	PWR+ (n = 50)	PWR+ (n = 100)	PWR+ (n = 1000)
3dB Beamwidth (deg.)	7.18	9.4	5.91	4.18	1.42
Delay (ms)	$4R + 125$	$4R + 36.0933$	$4R + 36.099$	$4R + 36.1011$	$4R + 36.1112$
$^1\Delta t$ (ms)	0	−88.9067	−88.901	−88.8989	−88.8888

[1] Δt refers to the total delay ($t_2 - t_1$, see Fig. 5(c)), with respect a 4 × 4 MIMO case. Negative values mean a shorter processing time than the referenced 4 × 4 case.
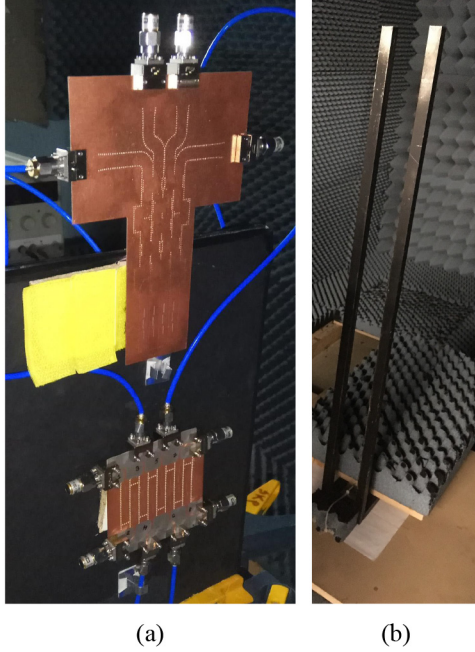
FIGURE 16. a) Radar transmitter defined by the SIW BM and antenna array (top) and the SIW receiver (bottom); b) Metallic posts employed as targets during the measurements.

FIGURE 17. Angular target response measurements where two targets are resolved using the *Pwr+* algorithm for different values of *n*. For these radar system measurements, targets were positioned at a distance of 2 meters from the radar and separated at the following angles (from the top to the bottom panel): ±5°, ±3°, ±2° and ±1°.

Angular target detection results which employed the Pwr_+ algorithm are reported in Fig. 17, where the two targets, with an angular separation equal to 10°, 6°, 4°, and 2° degrees, respectively, are considered. The gray lines show the independent SIMO views corresponding to an angular resolution of 30°, whereas the colored lines represent the resulting angular target response after applying Pwr_+ for different values of *n*. It should be noted that the resolution improves for increased *n*, as outlined in Table 4, and larger *n* marginally increases the total processing time, however, this is negligible as described in Section III-B (see also Table 4). This makes the proposed algorithm and beamformer a very convenient approach to decrease the total processing time while also offering enhanced angular resolution beyond comparable, and more classic, SIMO and MIMO radars with a similar number of RF chains, transmitters, and receivers.

Apart from an improvement in the detection of very close targets, the proposed radar system would also be able to cover a wider angular range due to the beamforming capabilities in comparison to the conventional SIMO and MIMO approaches. As is well known, the maximum detectable

range over angle is given by [62]:

$$R_{\max}(\theta) = \sqrt[4]{\frac{P_{\mathrm{t}} \cdot g(\theta)^2 \cdot \lambda^2 \cdot \sigma}{P_{\min} \cdot (4\pi)^3}} \quad [\mathrm{m}] \qquad (11)$$

where P_{t} is the transmitted power in watts (1 W, as a reference), $g(\theta)$ relates to the realized gain over angle in linear units, λ corresponds to the free-space wavelength (24.125 GHz), σ is the RCS of the target (in our case we take 100 m^2, which is the average value for a car), $P_{\min}$ relates to the minimum detectable power in watts needed for detection which is −82.8 dBm (whilst considering a signal-to-noise ratio of 5 dB) [29].

From this expression the realized gains and the maximum detectable range for the three relevant cases are shown in
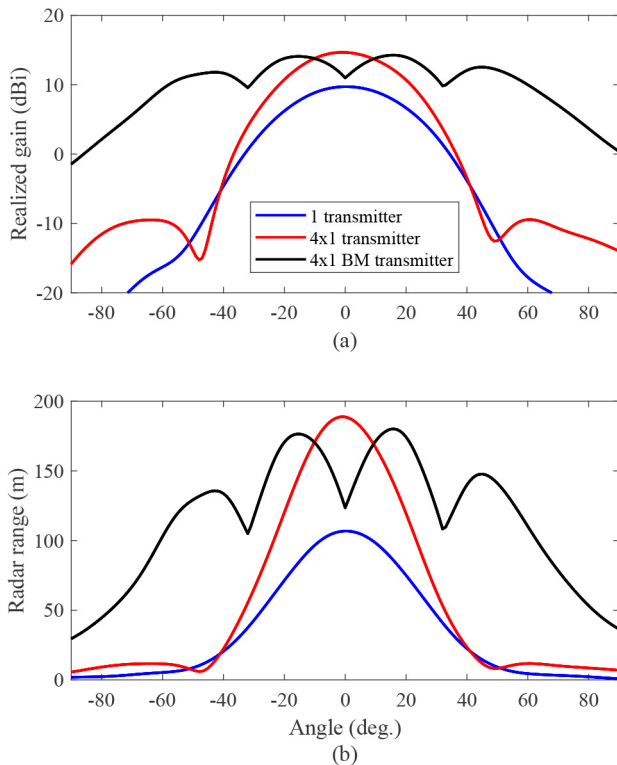
FIGURE 18. (a): Maximum realized gain versus angle for comparably sized radar transmitter antennas (representing SIMO and MIMO radars) and the BMA (representing the BM radar). (b): An estimation of the maximum detectable range versus angle by Eq. (11) whilst considering the different radar transmitters as in (a). Note: legend in (a) also applies to (b).

Fig. 18. These results include the radar transmitter patterns for the developed BMA as well as for comparably sized SIMO and MIMO radar transmitter antennas (see Fig. 18(a) and [35]). The black line corresponds to the proposed butler matrix transmitter (the envelope pattern), the red line relates to the same number of antennas, although equiphased by a corporate feeding network, and, the blue line corresponds to only one antenna at the transmitter. Clearly, the longest range over the widest possible angular range is exhibited by the BM radar. Although there are nulls at broadside and about ±30°, the maximum detectable range would still be over 100 meters (see Fig. 18(b)) which is more than enough time to compute the target and safely avoid it considering a car driving at its maximum (typically allowed) speed on a highway (120 km/h). This demonstrates that by using the proposed BM matrix radar, an important improvement in the FOV and maximum detectable range is achieved if compared to other arrangements; i.e., conventional SIMO and MIMO as reported herein.

VI. CONCLUSION

We have presented the design of a planar beamformer based on the use of an SIW-based Butler matrix associated with a processing technique defined as *Power Plus* (i.e., Pwr_+), to decrease the computational costs for FMCW radars. The passive Butler matrix beamformer at transmit has been integrated to achieve four independent beams and improves the angular resolution of the effective SIMO system without increasing the hardware complexity, the number of RF channels, the required radar signal processing as well as the encumbrance and cost of the developed structures.

The design of both the SIW Butler matrix and the corresponding radar antenna have been described and experimentally validated. Also, measurements within an anechoic chamber have been reported to describe the performance of the proposed radar. A good agreement between simulations and measurements has been observed. When compared to more conventional SIMO and MIMO FMCW radars, the proposed radar system also offers improvements in terms of higher signal-to-noise ratios, enhanced field-of-view, and higher returned signal powers which can increase the range of the radar.

The angular resolution and the total delay processing time of the proposed BM radar system, equipped with four receivers, defines a new type of 1×4 switched-beam FMCW radar architecture. This system has also been directly compared to a 4×4 MIMO radar. In particular, measurement results show that targets placed at an angular distance of up to 2° can be successfully detected using the proposed BM radar transmitter and the four-element receiver (which alone would have an angular resolution of 30°) while also providing shorter processing times when compared to more conventional radars. To achieve similar angular resolution, an alternative MIMO system would require a 7×8 radar configuration. This would significantly increase system complexity, processing and implementation costs. More importantly, it would unavoidably deteriorate the detection time, which is a key aspect for collision-avoidance applications and more real-time radars.

REFERENCES

[1] D. W. Bliss and K. W. Forsythe, "Multiple-input–multiple-output (MIMO) radar and imaging: Degrees of freedom and resolution," in *Proc. 37th Asilomar Conf. Signals Syst. Comput.*, vol. 1, Nov. 2003, pp. 54–59.

[2] E. Fishler, A. Haimovich, R. Blum, D. Chizhik, L. Cimini, and R. Valenzuela, "MIMO radar: An idea whose time has come," in *Proc. IEEE Radar Conf.*, Apr. 2004, pp. 71–78.

[3] I. Bekkerman and J. Tabrikian, "Target detection and localization using MIMO radars and sonars," *IEEE Trans. Signal Process.*, vol. 54, no. 10, pp. 3873–3883, Oct. 2006.

[4] A. M. Haimovich, R. S. Blum, and L. J. Cimini, "MIMO radar with widely separated antennas," *IEEE Signal Process. Mag.*, vol. 25, no. 1, pp. 116–129, Dec. 2007.

[5] E. Moldovan, S.-O. Tatu, T. Gaman, K. Wu, and R. G. Bosisio, "A new 94-GHz six-port collision-avoidance radar sensor," *IEEE Trans. Microw. Theory Techn.*, vol. 52, no. 3, pp. 751–759, Mar. 2004.

[6] S. M. Patole, M. Torlak, D. Wang, and M. Ali, "Automotive radars: A review of signal processing techniques," *IEEE Signal Process. Mag.*, vol. 34, no. 2, pp. 22–35, Mar. 2017.

[7] I. Bilik, O. Longman, S. Villeval, and J. Tabrikian, "The rise of radar for autonomous vehicles: Signal processing solutions and future research directions," *IEEE Signal Process. Mag.*, vol. 36, no. 5, pp. 20–31, Sep. 2019.

[8] C. Pfeffer, R. Feger, C. Wagner, and A. Stelzer, "FMCW MIMO radar system for frequency-division multiple TX-beamforming," *IEEE Trans. Microw. Theory Techn.*, vol. 61, no. 12, pp. 4262–4274, Dec. 2013.

[9] N. H. Lehmann, A. M. Haimovich, R. S. Blum, and L. Cimini, "High resolution capabilities of MIMO radar," in *Proc. 40th Asilomar Conf. Signals Syst. Comput.*, Oct. 2006, pp. 25–30.

[10] L. Anitori, A. Maleki, M. Otten, R. G. Baraniuk, and P. Hoogeboom, "Design and analysis of compressed sensing radar detectors," *IEEE Trans. Signal Process.*, vol. 61, no. 4, pp. 813–827, Feb. 2013.

[11] P. Van Dorp, R. Ebeling, and A. G. Huizing, "High resolution radar imaging using coherent multiband processing techniques," in *Proc. IEEE Radar Conf.*, 2010, pp. 981–986.

[12] E. M. Childers, "Method and system for obtaining high resolution 3-D images of moving objects by use of sensor fusion," U.S. Patent 7 672 504, Mar. 2, 2010.

[13] M. A. Herman and T. Strohmer, "High-resolution radar via compressed sensing," *IEEE Trans. Signal Process.*, vol. 57, no. 6, pp. 2275–2284, Jun. 2009.

[14] J.-J. Lin, Y.-P. Li, W.-C. Hsu, and T.-S. Lee, "Design of an FMCW radar baseband signal processing system for automotive application," *SpringerPlus*, vol. 5, no. 1, p. 42, 2016.

[15] G. Payá-Vayá and H. Blume, *Towards a Common Software/Hardware Methodology for Future Advanced Driver Assistance Systems* (Series in Transport Technology). Hannover, Germany: River, 2017, p. 133.

[16] S. Saponara, "Radar real-time image processing for machine perception," in *Real-Time Image Processing and Deep Learning*, vol. 10996. Bellingham, WA, USA: Int. Soc. Opt. Photon., 2019.

[17] K. Ogawa and A. Kajiwara, "2D high resolution of stepped-FM radar based on MUSIC scheme," in *Proc. IEEE Topical Conf. Wireless Sensors Sensor Netw.*, Jan. 2018, pp. 51–54.

[18] P. Stoica and A. Nehorai, "MUSIC, maximum likelihood, and Cramer–Rao bound: Further results and comparisons," *IEEE Trans. Acoust., Speech, Signal Process.*, vol. 38, no. 12, pp. 2140–2150, Dec. 1990.

[19] J. Capon, "High-resolution frequency-wavenumber spectrum analysis," *Proc. IEEE*, vol. 57, no. 8, pp. 1408–1418, Aug. 1969.

[20] S. Kim, D. Oh, and J. Lee, "Joint DFT-ESPRIT estimation for TOA and DOA in vehicle FMCW radars," *IEEE Antennas Wireless Propag. Lett.*, vol. 14, pp. 1710–1713, Apr. 2015, doi: 10.1109/LAWP.2015.2420579.

[21] S. Kim, B.-S. Kim, Y. Jin, and J. Lee, "Extrapolation-RELAX estimator based on spectrum partitioning for DOA estimation of FMCW radar," *IEEE Access*, vol. 7, pp. 98771–98780, 2019.

[22] W. F. Gabriel, "Spectral analysis and adaptive array superresolution techniques," *Proc. IEEE*, vol. 68, no. 6, pp. 654–666, Jun. 1980.

[23] P. J. Gething, *Radio Direction Finding and Superresolution*. London, U.K.: IET, 1991.

[24] S. Haykin *et al.*, *Radar Array Processing*. Berlin, Germany: Springer-Verlag, 1993. [Online]. Available: https://link.springer.com/book/10.1007/978-3-642-77347-1#about

[25] R. Mucci, "A comparison of efficient beamforming algorithms," *IEEE Trans. Acoust., Speech, Signal Process.*, vol. 32, no. 3, pp. 548–558, Jun. 1984.

[26] C. Liu, S. Liu, C. Zhang, Y. Huang, and H. Wang, "Multipath propagation analysis and ghost target removal for FMCW automotive radar," in *Proc. IET Int. Radar Conf.*, Chongqing, China, Nov. 2020, pp. 1–9.

[27] W. Wiesbeck and L. Sit, "Radar 2020: The future of radar systems," in *Proc. Int. Radar Conf. (Radar)*, 2014, pp. 1–6.

[28] B.-H. Ku *et al.*, "A 77–81 GHz 16-element phased-array receiver with ±50° beam scanning for advanced automotive radars," *IEEE Trans. Microw. Theory Techn.*, vol. 62, no. 11, pp. 2823–2832, Nov. 2014.

[29] M. I. Skolnik, *Introduction to Radar Systems*. New York, NY, USA: McGrawHill, 2001.

[30] A. G. Stove, "Linear FMCW radar techniques," *IEE Proc. Radar Signal Process.*, vol. 139, no. 5, pp. 343–350, 1992.

[31] J. Schäfer, M. Dittrich, H. Gulan, and T. Zwick, "Planar frequency scanning holographic antenna for FMCW-radar applications at 240 GHz," in *Proc. IEEE Int. Antennas Propag. Symp.*, 2016, pp. 1401–1402.

[32] M. Ettorre, R. Sauleau, L. Le Coq, and F. Bodereau, "Single-folded leaky-wave antennas for automotive radars at 77 GHz," *IEEE Antennas Wireless Propag. Lett.*, vol. 9, pp. 859–862, 2010.

[33] T. Djerafi and K. Wu, "A low-cost wideband 77-GHz planar Butler matrix in SIW technology," *IEEE Trans. Antennas Propag.*, vol. 60, no. 10, pp. 4949–4954, Oct. 2012.

[34] C. A. Alistarh *et al.*, "Millimetre-wave FMCW MIMO radar system development using broadband SIW antennas," in *Proc. 10th Eur. Conf. Antennas Propag.*, 2018, pp. 1–5.

[35] P. H. Re, C. Alistarh, S. Podilchak, G. Goussetis, J. Thompson, and J. Lee, "Millimeter-wave FMCW radar development using SIW Butler matrix for time domain beam steering," in *Proc. IEEE 16th Eur. Radar Conf.*, 2019, pp. 141–144.

[36] C. A. Alistarh, S. K. Podilchak, G. Goussestis, J. S. Thompson, and J. Lee, "Spectral smoothing by multiple radar pattern multiplication for improved accuracy," in *Proc. 18th Int. Symp. Antenna Technol. Appl. Electromagn. (ANTEM)*, 2018, pp. 1–9.

[37] J. Butler and R. Lowe, "Beam-forming matrix simplifies design of electronically scanned antennas," *Electron. Design*, vol. 9, no. 8, pp. 170–173, Apr. 1961.

[38] Q. Yang, Y. Ban, J. Lian, Z. Yu, and B. Wu, "SIW Butler matrix with modified hybrid coupler for slot antenna array," *IEEE Access*, vol. 4, pp. 9561–9569, 2016.

[39] S. Lutz, K. Baur, and T. Walter, "77 GHz lens-based multistatic MIMO radar with colocated antennas for automotive applications," in *IEEE Int. Microwave Symp. Dig.*, Jun. 2012, pp. 1–3.

[40] Y. J. Cho, G. Suk, B. Kim, D. K. Kim, and C. Chae, "RF lens-embedded antenna array for mmWave MIMO: Design and performance," *IEEE Commun. Mag.*, vol. 56, no. 7, pp. 42–48, Jul. 2018.

[41] T. Xie, L. Dai, X. Gao, H. Yao, and X. Wang, "On the power leakage problem in beamspace MIMO systems with lens antenna array," in *Proc. IEEE Veh. Technol. Conf.*, Sep. 2017, pp. 1–5.

[42] Y. Zeng and R. Zhang, "Millimeter wave MIMO with lens antenna array: A new path division multiplexing paradigm," *IEEE Trans. Commun.*, vol. 64, no. 4, pp. 1557–1571, Apr. 2016.

[43] S. Li, Z. N. Chen, T. Li, F. H. Lin, and X. Yin, "Characterization of metasurface lens antenna for sub-6 GHz dual-polarization full-dimension massive MIMO and multibeam systems," *IEEE Trans. Antennas Propag.*, vol. 68, no. 3, pp. 1366–1377, Mar. 2020.

[44] I. V. Komarov and S. M. Smolskiy, *Fundamentals of Short-Range FM Radar*. Boston, MA, USA: Artech House, 2003.

[45] J. K. Kauppinen, D. J. Moffatt, H. H. Mantsch, and D. G. Cameron, "Smoothing of spectral data in the Fourier domain," *Appl. Opt.*, vol. 21, no. 10, pp. 1866–1872, 1982.

[46] *IEEE Standard for Radar Definitions*, IEEE Standard 686-2017, 2017.

[47] R. Rouveure, P. Faure, M. Jaud, M. Monod, and L. Moiroux-Arvis, "Distance and angular resolutions improvement for a ground-based radar imager," in *Proc. IEEE Int. Radar Conf.*, 2014, pp. 1–6.

[48] A. Ganis *et al.*, "A portable 3-D imaging fmcw MIMO radar demonstrator with a 24 × 24 antenna array for medium-range applications," *IEEE Trans. Geosci. Remote Sens.*, vol. 56, no. 1, pp. 298–312, Jan. 2018.

[49] H. L. V. Trees, *Optimum Array Processing*. Hoboken, NJ, USA: Wiley, 2002, ch. 9, pp. 1142–1143.

[50] J. Blass, "Multidirectional antenna—A new approach to stacked beams," in *Proc. IRE Int. Convent. Rec.*, vol. 8, Mar. 1960, pp. 48–50.

[51] R. F. Gleason and R. M. Greene, "A wide-aperture HF direction-finder with sleeve antennas," Dept. Comput. Sci., U.S. Naval Res. Lab., Monterey, CA, USA, Rep. 843, Aug. 1958.

[52] T. MacNamara, "Simplified design procedures for butler matrices incorporating 90° hybrids or 180^{circ} hybrids," *IEE Proc. H Microwaves Antennas Propag.*, vol. 134, no. 1, pp. 50–54, Feb. 1987.

[53] H. Moody, "The systematic design of the Butler matrix," *IEEE Trans. Antennas Propag.*, vol. 12, no. 6, pp. 786–788, Nov. 1964.

[54] R. Elliott, "An improved design procedure for small arrays of shunt slots," *IEEE Trans. Antennas Propag.*, vol. 31, no. 1, pp. 48–53, Jan. 1983.

[55] R. Elliott and W. O'Loughlin, "The design of slot arrays including internal mutual coupling," *IEEE Trans. Antennas Propag.*, vol. 34, no. 9, pp. 1149–1154, Sep. 1986.

[56] S. E. Hosseininejad and N. Komjani, "Optimum design of traveling-wave SIW slot array antennas," *IEEE Trans. Antennas Propag.*, vol. 61, no. 4, pp. 1971–1975, Apr. 2013.

[57] A. J. Farrall and P. R. Young, "Integrated waveguide slot antennas," *Electron. Lett.*, vol. 40, no. 16, pp. 974–975, Aug. 2004.

[58] H. J. Riblet, "The short-slot hybrid junction," *Proc. IRE*, vol. 40, no. 2, pp. 180–184, Feb. 1952.

[59] L. T. Hildebrand, "Results for a simple compact narrow-wall directional coupler," *IEEE Microwave Guided Wave Lett.*, vol. 10, no. 6, pp. 231–232, Jun. 2000.

[60] D. Deslandes and K. Wu, "Design consideration and performance analysis of substrate integrated waveguide components," in *Proc. 32nd Eur. Microwave Conf.*, Sep. 2002, pp. 1–4.

[61] E. D. Caballero, A. B. Martinez, H. E. Gonzalez, O. M. Belda, and V. B. Esbert, "A novel transition from microstrip to a substrate integrated waveguide with higher characteristic impedance," in *Proc. IEEE Int. Microwave Symp. Dig.*, Jun. 2013, pp. 1–4.

[62] M. I. Skolnik, *Radar Handbook Second Edition*. New York, NY, USA: McGraw-Hill, 1990.

PASCUAL D. HILARIO RE was born in Murcia, Spain. He received the B.Eng. and M.Sc. degrees in telecommunications engineering from the Universidad Politcnica de Cartagena, Spain, in 2012 and 2015, respectively, and the Ph.D. degree from Heriot-Watt University, Edinburgh, U.K., in 2019.

His current research interests include retrodirective systems, wireless power transmission applications, automotive radar, and analysis and design of power amplifiers.

DAVIDE COMITE (Senior Member, IEEE) received the master's degree (*cum laude*) in telecommunications engineering and the Ph.D. degree in electromagnetics and mathematical models for engineering from the Sapienza University of Rome, Rome, Italy, in 2011 and 2015, respectively.

He is currently a Postdoctoral Researcher with the Sapienza University of Rome. From March 2014 to June 2014, he was a visiting Ph.D. student with the Institute of Electronics and Telecommunications of Rennes, University of Rennes 1, Rennes, France. In 2015, he was a Postdoctoral Researcher with the Center of Advanced Communications, Villanova University, Villanova, PA, USA. His scientific research interests include the study and design of leaky-wave antennas, 2-D periodic leaky-wave antennas, the generation of non-diffracting waves and pulses, the study of the scattering from natural surfaces, GNSS, reflectometry, and radar altimeter applications over the land. His interests also include microwave imaging and object detection performed through GPR, and the modeling of the radar signature in forward scatter radar systems. He was the recipient of a number of awards at national and international conferences. He was the recipient of the Young Scientist Award at URSI GASS 2020 and Publons Top Peer Reviewers Award for both Geoscience and Engineering in 2018, and for cross-fields in 2019. In 2020, he was awarded as the Best Reviewer for the IEEE JOURNAL OF SELECTED TOPICS IN APPLIED EARTH OBSERVATIONS AND REMOTE SENSING. In 2019 and 2020, he was recognized as an a Outstanding Reviewer of the IEEE TRANSACTIONS ON ANTENNAS AND PROPAGATION by the IEEE Antennas and Propagation Society. He is currently a reviewer for several international journals. He is also an Associate Editor for the *IET Journal of Engineering*, the *IET Microwaves, Antennas and Propagation*, and IEEE ACCESS. He is a Senior Member of URSI.

SYMON K. PODILCHAK (Member, IEEE) received the B.A.Sc. degree in engineering science from the University of Toronto, Toronto, ON, Canada, in 2005, and the M.A.Sc. and Ph.D. degrees in electrical engineering from Queen's University, Kingston, ON, Canada, in 2008 and 2013, respectively.

From 2013 to 2015, he was an Assistant Professor with Queen's University. In 2015, he joined Heriot-Watt University, Edinburgh, U.K., as an Assistant Professor, and became an Associate Professor in 2017. He is currently a Senior Lecturer with the School of Engineering, The University of Edinburgh, Edinburgh. He is also a Registered Professional Engineer and has had industrial experience as a Computer Programmer, and has designed 24 and 77 GHz automotive radar systems with Samsung and Magna Electronics. Recent industry experience also includes the design of high frequency surface-wave radar systems, professional software design and implementation for measurements in anechoic chambers for the Canadian Department of National Defence and the SLOWPOKE Nuclear Reactor Facility. He has also designed compact antennas for wideband military communications, highly compact circularly polarized antennas for CubeSats with COM DEV International and The European Space Agency, and new wireless power transmission systems for Samsung. His research interests include surface waves, leaky-wave antennas, metasurfaces, UWB antennas, phased arrays, and RF integrated circuits.

Dr. Podilchak and his students were the recipient of many best paper awards and scholarships, most notably Research Fellowships from the IEEE Antennas and Propagation Society (AP-S), the IEEE Microwave Theory and Techniques Society (MTT-S), the European Microwave Association, and six Young Scientist Awards from the International Union of Radio Science. He was also the recipient of the Postgraduate Fellowship from the Natural Sciences and Engineering Research Council of Canada. In 2011, 2013, and 2020, he and his students received Student Paper Awards at the IEEE International Symposium on Antennas and Propagation and the Best Paper Prize for Antenna Design at the European Conference on Antennas and Propagation in 2012, for his work on CubeSat antennas, and he was the recipient of the European Microwave Prize for his research on surface waves and leaky-wave antennas in 2016. In 2017 and 2019, he was bestowed a Visiting Professorship Award at Sapienza University, Rome, Italy, and from 2016 to 2019, his research was supported by a H2020 Marie Skłodowska-Curie European Research Fellowship. He was also the recipient of the Outstanding Dissertation Award for his Ph.D. He was recognized as an Outstanding Reviewer of the IEEE TRANSACTIONS ON ANTENNAS AND PROPAGATION, in 2014 and 2020. He was also the Founder and a First Chairman of the IEEE AP-S and IEEE MTT-S Joint Chapters in Canada and Scotland, in 2014 and 2019. In recognition of these services, he was presented with an Outstanding Volunteer Award from IEEE in 2015, and in 2020, MTT-S recognized this Scotland Chapter for its activities and it was awarded the winner of the Outstanding Chapter Award. He has also served as a Lecturer for the European School of Antennas and an Associate Editor for the *IET Electronics Letters*. He is currently a Guest Associate Editor of the IEEE OPEN JOURNAL OF ANTENNAS AND PROPAGATION and IEEE ANTENNAS AND WIRELESS PROPAGATION LETTERS.

CRISTIAN A. ALISTARH (Student Member, IEEE) received the M.Eng. degree in electronics and computer science from the University of Edinburgh in 2015, as a Keycom Scholar, the joint M.Sc. degree in sensors and imaging systems with the University of Glasgow and University of Edinburgh, sponsored by the Scottish Council, U.K. He is currently pursuing the joint Ph.D. degree with Heriot-Watt University and the University of Edinburgh in partnership with Samsung Research and Development, South Korea.

His research interests include: high resolution automotive radar, MIMO systems, digital beamforming, sparse antenna design, and compressed sensing. In April 2018, he was shortlisted for "Best Paper in Antenna Design and Applications" at the European Conference in Antennas and Propagation and also in the same year in August he won 1st Place in the Student Paper Competition at the International Symposium on Antenna Technology and Applied Electromagnetics (ANTHEM), Waterloo, Canada. In 2019, he was also awarded the European Microwave Association Internship Award leading to a research placement at TNO Research and Defence in the Netherlands, which was completed successfully in September 2020. He is a member of the IEEE Antennas and Propagation Society (AP-S), IEEE Microwave Theory and Techniques Society (MTT-S), and IEEE Electron Devices Society. He is also the Secretary for the IEEE AP-S and MTT-S Joint Scottish Chapter, which won the 2020 Outstanding Chapter Award by MTT-S. He is also a reviewer for IEEE.

MATHINI SELLATHURAI (Senior Member, IEEE) is currently a Professor of Signal Processing and Wireless Communications and the Dean of Science and Engineering with Heriot-Watt University, Edinburgh, U.K. She has been active in signal processing research for the past 20 years and has a strong international track record in multiple-input, multiple-output (MIMO) signal processing with applications in radar, and wireless communications. She held visiting positions with Bell-Laboratories, Holmdel, NJ, USA, and The Canadian Communications Research Centre, Ottawa, Canada. She has published over 200 peer reviewed papers in leading international journals and IEEE conferences, given invited talks and has written several book chapters as well as a research monograph as a Lead Author. Her present research includes full-duplex systems, passive radar topography, localization, massive-MIMO, non-orthogonal multiple access, waveform designs, caching technologies, assisted care technologies, IoT, hearing-aids, optimal coded-modulation designs using auto-encoders, channel prediction, and mm-wave imaging and communications. She is a recipient of an IEEE Communication Society Fred W. Ellersick Best Paper Award in 2005, the Industry Canada Public Service Awards for contributions to Science and Technology in 2005, and Awards for contributions to Technology Transfers to Industry in 2004. She was the recipient of the Natural Sciences and Engineering Research Council of Canada Doctoral Award for her Ph.D. dissertation in 2002. She was an Editor for IEEE TRANSACTIONS ON SIGNAL PROCESSING from 2009 to 2014, and from 2015 to 2018, the General Co-Chair of IEEE SPAWC2016 in Edinburgh, and a member for IEEE SPCOM Technical Strategy Committee from 2014 to 2019.

GEORGE GOUSSETIS (Senior Member, IEEE) received the Diploma degree in electrical and computer engineering from the National Technical University of Athens, Greece, in 1998, the B.Sc. degree (Hons.) in physics from University College London, London, U.K., in 2002, and the Ph.D. degree from the University of Westminster, London, U.K., in 2002.

In 1998, he joined Space Engineering, Rome, Italy, as an RF Engineer. In 1999, he was a Research Assistant with the Wireless Communications Research Group, University of Westminster. From 2002 to 2006, he was a Senior Research Fellow with Loughborough University, Loughborough, U.K. He was a Lecturer (Assistant Professor) with Heriot-Watt University, Edinburgh, U.K., from 2006 to 2009, and a Reader (Associate Professor) with Queen's University Belfast, U.K., from 2009 to 2013. In 2013, he joined Heriot-Watt, as a Reader, and was promoted to a Professor in 2014. He has authored or coauthored more than 200 peer-reviewed papers, five book chapters, one book, and two patents. His research interests include the modeling and design of microwave filters, frequency-selective surfaces and periodic structures, leaky wave antennas, microwave sensing, and curing as well numerical techniques for electromagnetics. He was the co-recipient of the 2011 European Space Agency Young Engineer of the Year Prize, the 2011 EuCAP Best Student Paper Prize, the 2012 EuCAP Best Antenna Theory Paper Prize, and the 2016 Bell Labs Prize. He has held a Research Fellowship with the Onassis Foundation in 2001, a Research Fellowship with the U.K. Royal Academy of Engineering from 2006 to 2011, and a European Marie-Curie Experienced Researcher Fellowship from 2011 to 2012.

JOHN THOMPSON (Fellow, IEEE) received the Ph.D. degree in electrical engineering from University of Edinburgh, Edinburgh, U.K., in 1995.

He is currently a Professor with the School of Engineering, University of Edinburgh. He currently participates in two U.K. research projects, which study new concepts for signal processing and next-generation wireless communications. He has authored or coauthored in excess of 350 papers on the topics of his research interests, which include antenna array processing, cooperative communications systems, energy efficient wireless communications, and their applications. He was the Co-Chair of the IEEE Smart Gridcomm Conference held in Aalborg, Denmark. In January 2016, he was elevated to Fellow of the IEEE for contributions to antenna arrays and multihop communications. From 2015 to 2018, he was recognized by Thomson Reuters as a Highly Cited Researcher.

JAESUP LEE received the M.S. degree in electrical engineering from the University of California at Los Angeles, Los Angeles, CA, USA.

He is currently with the Samsung Advanced Institute of Technology, Suwon, South Korea. His current interests include RF and analog circuits, especially ultralow-power personal network platforms, and RF wireless power transfer.